A COMPARISON BETWEEN THE VARIABILITY STRUCTURE OF THE REMOTELY SENSED SEA-SURFACE TEMPERATURE AND PIGMENT DISTRIBUTIONS

Mati Kahru
Institute of Thermophysics and Electrophysics,
Estonian Academy of Sciences
Paldiski Rd. 1, Tallinn 200031
USSR
Commission VII

Introduction

Since the work of Platt (1972) spectral analysis has been widely used for the interpretation of the plankton variability in the ocean. It has been assumed that the shape of the variance spectra (e.g. its slope in the log-log plot in relation to wavenumber k) can provide clues to discover the mechanisms, governing the distribution of plankton. After the initial flush of papers (Denman and Platt, 1975; Denman, 1976 and many others) the enthusiasm gradually decreased. Initial theories, set forth to explain the variance spectra of chlorophyll (index of phyto-plankton abundance) gave inconsistent results. Some theories (Denman and Platt, 1976; Denman et al., 1977) predicted a brake from shallower to steeper slopes with increasing wavenumbers. Another (Fasham, 1978), on the contrary, predicted flattening of the chlorophyll spectrum with increasing wavenumbers for a positive net growth rate. Platt (1978) concluded that if there was any merit in the concept of a spectral break at a critical wavenumber, the length of transects commonly used by shipboard patchiness studies was not sufficient. At the same time, the imagery of the Coastal Zone Color Scanner (CZCS), the principal source of synoptic maps of the "chlorophyll-like" pigments (Gordon and Morel, 1983), has not been studied by spectral analysis in a systematic way. By comparison, a number of papers have dealt with the variability structure of the sea surface temperature (SST) distributions obtained from the Advanced Very High Resolution Radiometer (AVHRR) (Deschamps et al., 1981). It has been argued (Lesieur and Sadourny, 1981; Fasham, 1978; Army and Flament, 1985) that spectral slopes per se are only weak constraints for testing theories on the structure of flows or the control of phytoplankton patchiness. In this regard, comparison of the pigment and SST spectra should yield more meaningful information.

In this paper the spatial variance spectra of the near-surface pigment concentrations (from CZCS) and SST (from AVHRR) are analyzed. Most of the images originate from the California Current area, a few from the North and the Baltic Seas.

Methods

The CZCS and AVHRR images were processed at the Jet Propulsion Laboratory (Pasadena, California) by M. Abbott and P. Zion using software developed in the University of Miami (Abbott and Zion, 1985). After correction for geographic errors, a 1024-by-1024 pixel array was removed from each satellite pass. Geophysical algorithms were then applied to derive SST and near-surface chlorophyll-like pigments. SST was estimated using

the channel 4 (10 to 11.5 um) brightness temperature. The pigment concentration was derived using the Gordon algorithms (Gordon and Morel, 1983) as implemented in the Miami software. With both the SST and pigment concentrations, small absolute errors do not concern us since for spectral calculations only the relative spatial patterns are important. The SST and pigment images were then resampled and remapped to an equal area of 512-by-512 pixels. The remapped arrays have an approximate grid size of 1.1 x 1.1 km and are directly comparable over time and between sensors.
Series of parallel transects were extracted in the north-to-south and/or west-to-east directions from cloud-free areas. The distance between neighboring transects was usually 5 pixels. Each series contained up to 75 transects of equal length. The transects were trend corrected and tapered with the split cosine bell. The spectra were calculated with FFT and the Parzen lag window using FORTRAN subroutines from the NAGFLIB

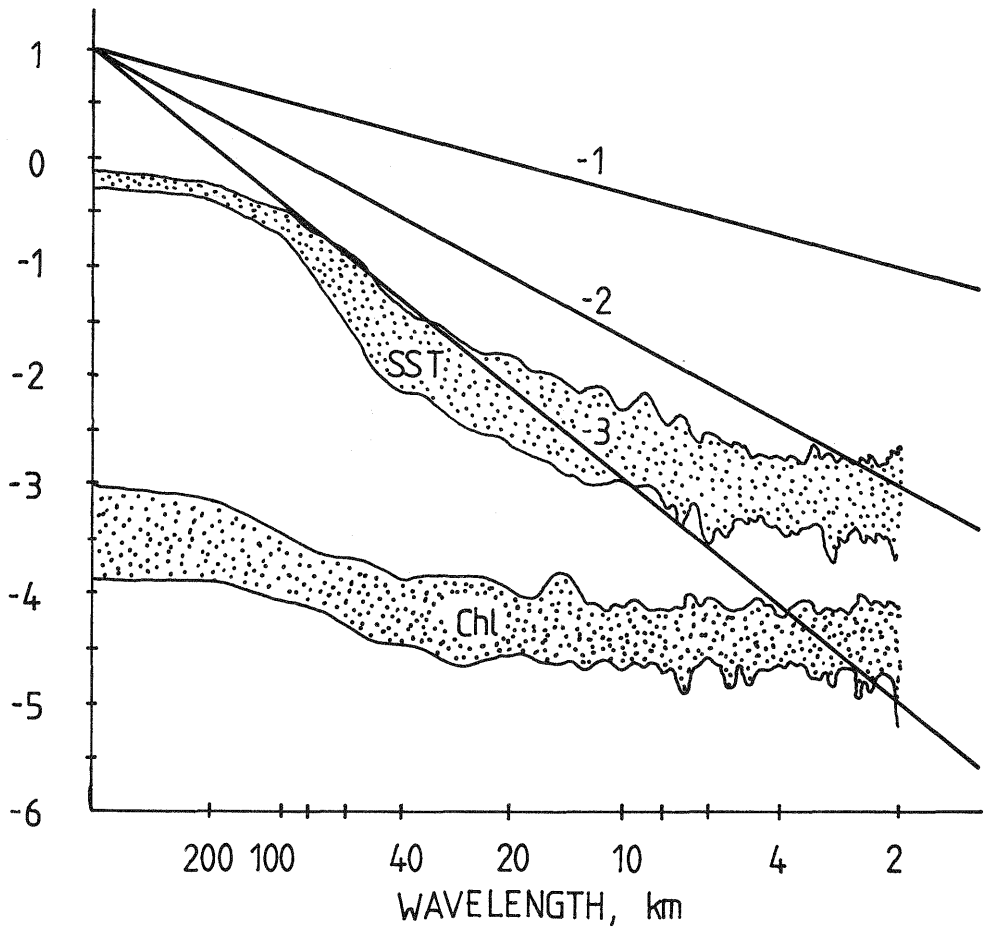

Fig. 1. Envelopes of the variance spectra of temperature (SST) and pigment concentration (Chl) for 28 parallel north-south transects in the California current area, 2 November 1981.

package. The calculation of bivariate spectra was similar in principle, the final results being the squared coherency spectrum estimates with their confidence bounds at the 95% level. Due to the finite length and resolution of the transects, the spectra are reliable for the wavelength range of 2-100 km. The variance spectra were integrated in several wavenumber bands, yielding a decomposition of the total variance into contributions at different scales. The mean spectral slopes were then calculated between these bands. All of the statistics were averaged over sets of parallel transects or spectra.

Autospectra of pigment and SST spatial variance

A characteristic feature of the pigment data was an obvious increase in variance with the increase of the mean pigment concentration. The SST data showed no relationship between the mean and variance. Examples of the spectra of spatial variance are shown on Fig. 1. with the statistics given in Tables 1, 2.

Table 1. Statistics of the sets of phytoplankton pigment spectra calculated from parallel transects from the California Current (CC) and other areas.

Area	Date (yy-mm-dd)	Mean [mg/m3]	Mean spectral slopes in wavelength ranges in km 73.3-10.5	10.0-2.2	73.3-2.2
CC	81-04-04	0.29	-2.42	-1.89	-2.08
CC	81-04-04	0.28	-2.05	-2.05	-1.99
CC	81-04-04	0.31	-1.75	-2.08	-1.96
CC	81-04-21	0.46	-1.81	-0.05	-0.94
CC	81-05-08	0.09	-2.08	-0.08	-1.15
CC	81-05-08	0.01	-2.19	-0.26	-1.36
CC	81-05-08	1.60	-2.84	-2.16	-2.39
North Sea	80-06-06	1.36	-2.42	-0.84	-1.44
North Sea	80-06-06	1.25	-2.42	-0.25	-1.33
CC	81-06-15	0.08	-0.88	-0.41	-0.50
CC	81-06-15	0.08	-1.68	-0.13	-0.78
CC	81-06-16	0.05	-1.00	0.10	-0.43
CC	81-06-16	0.05	-1.36	-0.01	-0.72
Baltic	79-06-19	1.61	-0.63	-0.87	-0.63
Baltic	79-06-19	2.13	-0.93	-0.67	-0.74
CC	81-07-07	1.00	-2.13	-2.37	-2.33
CC	81-07-08	1.10	-2.43	-2.24	-2.36
CC	81-11-02	0.08	-0.75	-0.07	-0.34
CC	81-11-02	0.09	-1.43	-0.01	-0.67
CC	81-11-02	0.08	-0.85	-0.10	-0.46
CC	81-11-03	0.14	-0.93	0.04	-0.42
CC	81-11-03	0.14	-1.00	0.16	-0.45
CC	81-11-03	0.18	-1.65	0.03	-0.79
CC	81-11-03	0.17	-1.80	-0.24	-0.89
	Mean:	0.53	-1.64	-0.69	-1.13

All the SST spectra were quite similar in shape with steep slopes flattening with the increase of wavenumbers. The pigment spectra were much more variable but both seemed to have a bimodal distribution of the slopes (Fig. 2), corresponding to

the presence or absence of offshore filaments ("squirts" or "jets") in the California current (see Abbott and Zion, 1985). Steep pigment spectra (slopes -2...-2.5) corresponded to transects across systems of filaments and were associated with higher mean concentration. In case of oligotrophic conditions with low pigment levels and low variability, the pigment spectra were close to the white noise spectrum (slopes between 0 and -1). Surprisingly, the two pigment spectra from the Baltic Sea were also almost flat (slopes between -0.5 and -1). From many in situ transects of pigment and plankton concentration in the Baltic (Kahru, unpublished) there has been no evidence of this kind of flat spectra. Therefore the Baltic Sea data must be treated with caution as the algorithms of pigment retrieval were not reliable for Morel Case 2 waters (Gordon and Morel, 1985). In 70% of the cases, the SST spectra were significantly steeper (in the wavelength range 73.3-2.2 km) than the corresponding pigment spectra, and for the rest the difference in the slopes was insignificant.

Only a few sets of pigment spectra happened to be consistent with the Platt-Denman prediction of the spectra steepening towards the smaller scales. On the contrary, most of the pigment spectra (22 of 24 sets) became shallower and not steeper along wavelengths from 73.3 to 4.5 Km. The same was true for most of the SST spectra (16 out of 17 sets). Between the wavelengths from 31.4 to 2.2 km the averaged spectral slopes flattened for 66% of the pigment spectra and for 94% of the SST spectra. The grand mean slope monotonously flattened with increasing wavenumbers.

Table 2. Statistics of the sets of SST spectra calculated from parallel transects from the California current area.

Date (yy-mm-dd)	Mean [C·]	Mean spectral slopes in wavelength ranges in km 73.3-10.5	10.0-2.2	73.3-2.2
81-04-04	7.19	-1.84	-1.06	-1.59
81-04-21	9.44	-2.26	-0.65	-1.60
81-05-07	10.22	-2.94	-1.03	-2.28
81-05-08	10.31	-2.56	-0.39	-1.70
81-05-09	10.75	-2.10	-1.55	-1.83
81-05-09	11.43	-2.51	-0.33	-1.52
81-06-16	15.13	-2.39	-1.81	-1.94
81-06-16	15.01	-2.74	-0.13	-1.54
81-07-08	13.16	-2.72	-1.08	-2.32
81-07-08	11.66	-2.97	-0.98	-2.32
81-07-10	12.59	-2.85	-1.14	-2.22
81-07-12	12.59	-2.51	-1.10	-2.04
81-07-15	12.77	-3.10	-0.93	-2.30
81-11-02	18.42	-2.51	-0.58	-1.66
81-11-03	18.65	-2.47	-0.93	-1.68
81-11-03	17.78	-2.38	-0.35	-1.48
81-11-03	18.18	-2.56	-0.39	-1.64
Mean:	13.25	-2.55	-0.85	-1.86

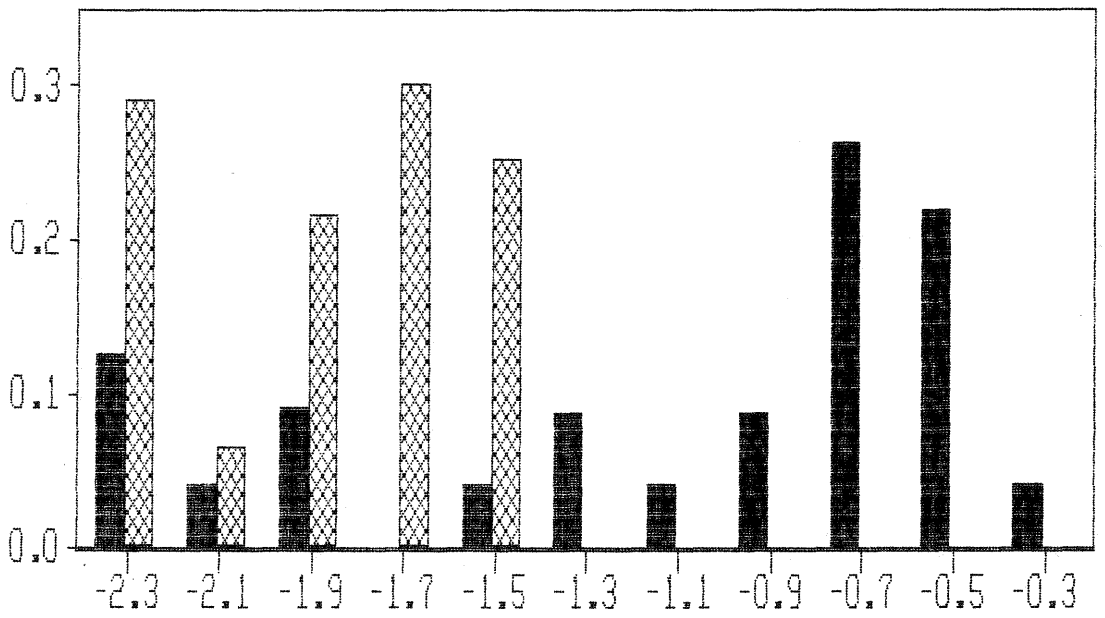

Fig. 2. Frequency histograms of pigment (solid) and SST (hatched) spectral slopes from the CC area in the wavelength band 73.3-2.2 km.

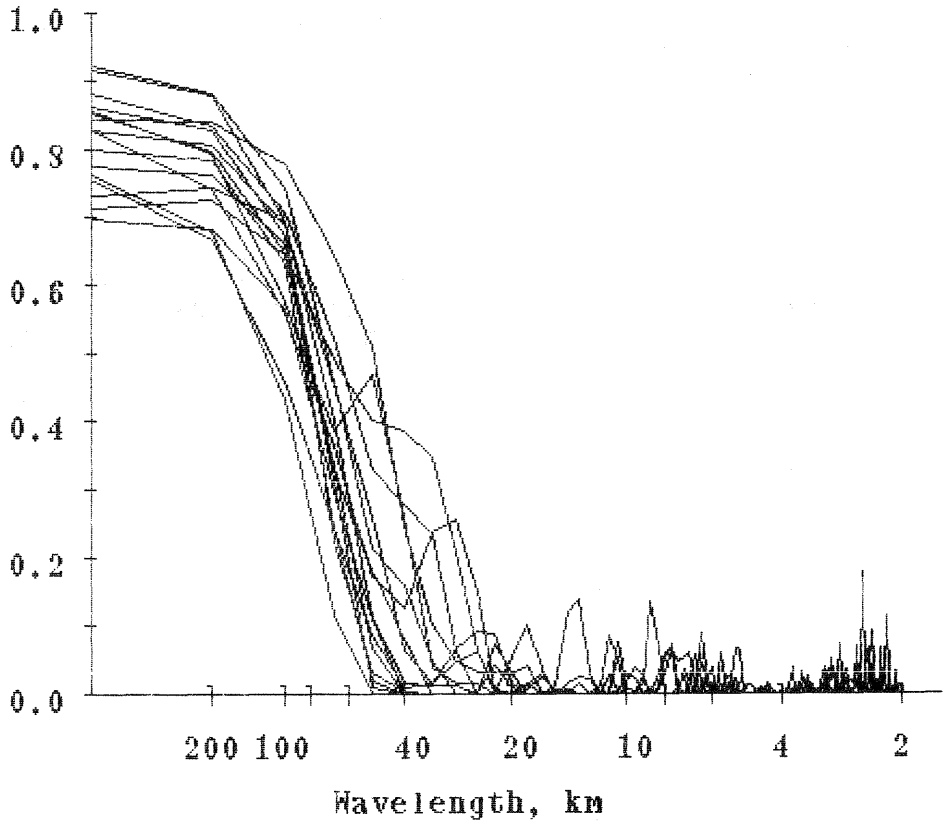

Fig. 3. Lower 95% confidence limits of the squared coherency spectra between pigment and SST patterns from 16 north-south transects in the California current area, 8 July 1981.

Coherence between the pigment and SST distributions

A general feature of the squared coherency spectra between the pigment and SST distributions in the California current area was their significant coherency on the longer wavelengths, and a drop to nonsignificant or spurious coherency starting from some characteristic wavelength (Fig. 3). Averaging over each set of spectra, I calculated the minimal coherence length (hereafter, coherence length), defined as the mean wavelength at which the lower 95% confidence limits of the coherency spectra first reach zero when moving from lower towards higher wavenumbers. For a few pairs of transects where the coherency was insignificant even at the longest scales, the coherence length was assumed to be equal to the length of the transects. The coherence lengths for pairs of pigment and SST images ranged from 27.6 km to over 500 km (Table 3). As could be expected, the coherence length is inversely related to the squared coherency at longer wavelengths. Although structures with wavelengths below the coherence length (e.g. fronts) may have a one-to-one correspondence between the distributions of pigments and SST, on the average, only the longer wavelengths are significantly correlated. The shortest coherence lengths belong to sets of north-south transects across the cross-shelf filaments in the California current system, the longest - to the oligotrophic oceanic conditions. In case of the filaments, coherency is highly anisotropic: higher across the filaments than along the filaments (cf. coherence lengths 172 vs. 321 km). In case of the low-variability conditions, coherency is isotropic (cf. coherence lengths 330 vs. 389 km). The squared coherency is obviously higher when more variance is present on longer scales. The same relationship is manifest in the significant correlation between the coherence length and the

Table 3. Characteristics of the squared coherency spectra, averaged over sets of spectra, for pairs of pigment and SST images from the California Current area.

Date (yy-mm-dd)	Time lag (h)	Coherence length (km)	Squared coherency on the following wavelengths: 73.3 km	31.4 km	20.0 km	14.7 km
81-04-04	7	74.6	0.24	0.33	0.27	0.25
81-04-21	7	341.1	0.14	0.13	0.12	0.24
81-05-08	40	87.4	0.45	0.26	0.24	0.17
81-05-08	7	172.5	0.29	0.30	0.24	0.17
81-05-08	7	320.9	0.16	0.25	0.21	0.19
81-06-16	4	330.1	0.17	0.14	0.10	0.10
81-06-16	4	388.6	0.25	0.15	0.12	0.12
81-07-07	8	30.5	0.76	0.52	0.35	0.15
81-07-08	4	27.6	0.81	0.52	0.35	0.31
81-11-02	3	382.9	0.11	0.11	0.12	0.12
81-11-03	4	376.7	0.18	0.16	0.12	0.10
81-11-03	4	536.3	0.14	0.18	0.09	0.14
81-06-15	20	416.8	0.15	0.11	0.09	0.09
Average:	9.2	268.2	0.30	0.24	0.19	0.17
Minimum:	3	27.6	0.11	0.11	0.09	0.09
Maximum:	40	536.3	0.81	0.52	0.35	0.31

spectral slopes of the pigment and SST autospectra. The general relationship is: the more variance there is on the longer scales, the steeper the autospectra, the higher the coherency, and the smaller the coherence length.

To determine the influence of the time lag between the pigment and SST distributions, the decorrelation between a pigment image and a sequence of SST images with increasing time separation was examined. All of the image sequences happened to be from the high variability situations. The decrease of coherency with increasing time separation looks rather regular (Fig. 4): a fast decorrelation period during the first 2 days followed by a slower decrease in the next days. The nearly linear trends could be used to correct all the pigment/SST coherence data to zero time lags. However, the assumption of equal decorrelation rate cannot be substantiated for different conditions. It is likely that the time separation between pigment and the corresponding SST images was not a major cause for the comparatively low coherency.

A few calculations of the squared coherency between successive pigment images showed the same general relationship: higher coherency and lower coherence length with higher mean concentration and higher variance. For the time lag of 1 day the coherence length for successive pigment images ranged from about 40 km to more than 300 km.

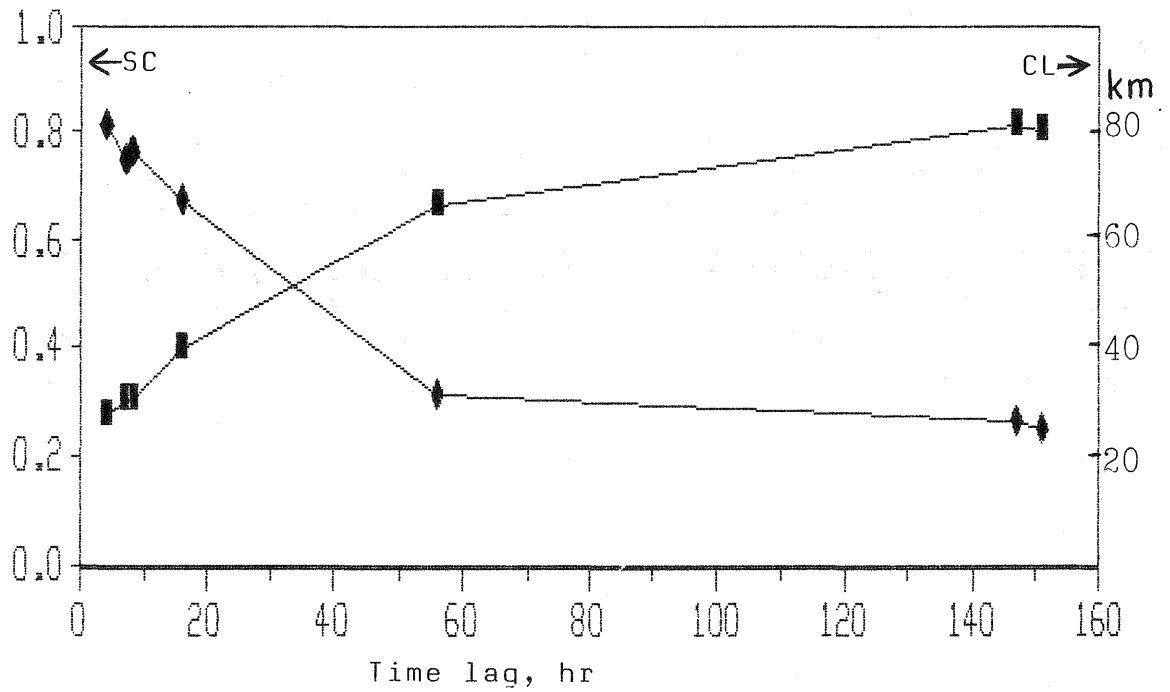

Fig. 4. Decorrelation of pigment and SST patterns with increasing time separation: decrease of the squared coherency (SC) and increase of the coherence length (CL). The data points are connected for sake of clarity, they are not all from the same sequence of images.

Discussion

The pigment variance spectra, obtained here from the CZCS images, are in a number of ways different from the majority of spectra, obtained from shipboard chlorophyll measurements on shorter length scales. For example, 58% of the sets of pigment spectra, mostly from the oligotrophic conditions, had mean slopes between 0 and -1. It is important but by no means easy to distinguish between the real world and the artificial effects of data processing on the calculated spectra.

The data set from the California Current area clearly shows the existence of two hydrographic regimes. The regime with the offshore filaments is characterized by higher mean pigment concentration, high pigment variability on longer space scales, steep pigment and SST spectra, higher squared coherency between SST/pigment and successive pigment patterns, and shorter coherence lengths. The second regime represents typical oceanic (oligotrophic) conditions and has low mean pigment level and low pigment variability, especially on longer space scales. The coherency with the respective SST patterns and ensuing pigment images is low, and the coherence length is >300 km. It is clear that the signal to noise ratio of the CZCS algorithms deteriorates in case of very low pigment concentrations. If the noise was primarily on high frequencies, this could tend to flatten the spectra. At the same time, the "-1" power law is also predicted by Bennett and Denman (1985) as the equilibrium after a sufficiently long time lag from an initial perturbation. This is certainly consistent with the California Current data where the offshore moving filaments of nutrient-rich water are probably the most important perturbations. It could be conjectured that after the initial input of nutrients by the filaments, most of the pigment variance is generated on the longer space scales (≈10-100 km), resulting in "red" variance spectra (power laws "-2" and steeper). Subsequent stirring and mixing cause the pigment variance to cascade to ever higher wavenumbers, leading to "-1" spectra. The further flattening of the pigment spectra could be the effect of high-frequency noise from measurement and processing errors at low pigment concentrations. Chlorophyll transects with very low large-scale variability have also been observed by in situ measurements in Lake Tahoe (Abbott et al., 1982). Thus, apart from measurement errors, "noisy" pigment variance spectra with low large-scale variability may be typical for equilibrium-like conditions, away from strong nutrient inputs. In these conditions the SST need not carry any information about the nutrient status of the water, thus, resulting in low coherence between the SST and pigment patterns. In fact, many of the large scale pigment patterns of the "oligotrophic" cases that did not match the SST patterns looked quite real. In the high variability case the coherency between the pigment and SST patterns is not different from that between successive SST patterns with a similar time separation. In cases of negligible pigment/SST coherency the SST/SST coherency, though also lower, remains significant.

Acknowledgements. The author is indebted to M.R. Abbott and P.M. Zion for providing the images and to M.R. Abbott and K.L. Denman for helpful discussions.

References

Abbott M.R., T.M. Powell and P.J. Richerson (1982). The relationship of environmental variability to the spatial patterns of phytoplankton biomass in Lake Tahoe. J. Plankton Res., 4, 927-941.

Abbott M.R. and P.M. Zion (1985). Satellite observations of phytoplankton variability during an upwelling event. Cont. Shelf Res., 4, 661-680.

Armi L. and P. Flament (1985). Cautionary remarks on the spectral interpretation of turbulent flows. JGR, 90, 11779-11782.

Bennett A.F. and K.L. Denman (1985). Phytoplankton patchiness: inferences from particle statistics. J. Mar. Res., 43, 307-335.

Denman K.L. (1976). Covariability of chlorophyll and temperature in the sea. Deep Sea Res., 23, 539-550.

Denman K.L. and T. Platt (1975). Coherences in the horizontal distributions of phytoplankton and temperature in the upper ocean. Mem. Soc. roy. sci. Liege, 6th series, 7, 19-30.

Denman K.L. and T. Platt (1976). The variance spectrum of phytoplankton in the ocean. J. Mar. Res., 34, 593-601.

Denman K.L., A. Okubo and T. Platt (1977). The chlorophyll fluctuation spectrum in the sea. Limnol. Oceanogr., 22, 1033-1038.

Deschamps P.Y., R. Frouin and L. Wald (1981). Satellite determinations of the mesoscale variability of the sea surface temperature. J. Phys. Oceanogr., 11, 864-870.

Fasham M.J. (1978). The statistical and mathematical analysis of plankton patchiness. Ann. Rev. Oceanogr. Mar. Biol., 16, 43-79.

Gordon H.R. and A.Y. Morel (1983). Remote assessment of ocean color for interpretation of satellite visible imagery: a review. Springer-Verlag, N.Y., 114 pp.

Lesieur M. and R. Sadourny (1981). Satellite-sensed turbulent ocean structure. Nature, 294, 673.

Platt T. (1972). Local phytoplankton abundance and turbulence. Deep-Sea Res., 19, 183-187.

Platt T. (1978). Spectral analysis of spatial structure in phytoplankton populations. In: Spatial pattern in plankton communities, J. H. Steele, editor, Plenum, New York, pp. 73-84.